This article has been accepted for publication in a future issue of this journal, but has not been fully edited. Content may change prior to final publication. Citation information: DOI 10.1109/JSEN.2016.2578440, IEEE Sensors Journal

Integration of Fractal Biosensor in a Digital Microfluidic Platform

Yousof Mashraei, Shilpa Sivashankar, Ulrich Buttner

Abstract— **The digital microfluidic (DMF) platform introduces many applications in biomedical assays. If it is to be commercially available to the public, it needs to have the essential features of smart sensing and a compact size. In this work, we report on a fractal electrode biosensor that is used for both droplet actuation and sensing C-reactive protein (CRP) concentration levels to assess cardiac disease risk. Our proposed electrode is the first two-terminal electrode design to be integrated into DMF platforms. A simulation of the electrical field distribution shows reduced peak intensities and uniform distribution of the field. When compared to a V-notch square electrode, the fractal electrode shows a superior performance in both aspects, i.e. field uniformity and intensity. These improvements are translated into a successful and responsive actuation of a water droplet with 100V. Likewise, the effective dielectric strength is improved by a 33% increase in the fractal electrode breakdown voltage. Additionally, the capability of the fractal electrode to work as a capacitive biosensor is evaluated with CRP quantification test. Selected fractal electrodes undergo a surface treatment to immobilize anti-CRP antibodies on their surface. The measurement shows a response to the added CRP in capacitance within three minutes. When the untreated electrodes were used for quantification, there was no significant change in capacitance, and this suggested that immobilization was necessary. The electrodes configuration in the fabricated DMF platform allows the fractal electrodes to be selectively used as biosensors, which means the device could be integrated into point-of-care applications.**

Index Terms— **C-reactive protein, digital microfluidics, electrowetting on dielectric, fractal capacitor**

I. Introduction

IN THE face of advancing technology, devices used in daily life (such as smart phones) are becoming more compact and are offering a wider range of uses. However, medical services are still not being efficiently integrated within them. It is not feasible to inset sophisticated sensors into these devices due to the high cost and low reliability of these sensors. Although special gadgets are emerging solely to provide certain bioassay, more effort is still needed to widen their scope to include more biomedical assays and chemicals [1-3]. Nonetheless, the world is demanding adequate healthcare services that are able to prevent devastating health problems through early diagnosis. For this reason, medical diagnostic systems have to be miniaturized, easy-to-use, cost efficient, and capable of providing faster bioassays. One technology that can potentially meet these needs is the digital microfluidic (DMF) system [4]. The DMF platform, which is a Lab-on-a-Chip (LOC) system that utilizes electrowetting on dielectric (EWOD) effect to perform droplet operations, is deployed in many biomedical applications [5-7]. It performs parallel operations, reduces the reagents' doses, and digitizes the process with addressable array configuration [8-12]. Nonetheless, DMF has several challenges that limit its use, such as the dielectric failures that comes with high voltage requirements [13-16] and the absence of integrated smart sensing in the DMF platform [17-21]. In this work we try to overcome these challenges by utilizing a novel electrode shape that requires less voltage and works as a sensor in order to allow smart sensing in the DMF platform. Droplet actuation is the main core function of the DMF platform. Responsive droplet actuation is necessary for bioassays. To improve it, different electrode shapes with notches [22], wavy structures [23], or irregular shape[24] have been reported. However, all reported electrodes are fundamentally one-terminal electrodes and are almost exclusively used for actuation. Also, the use of high dielectric materials proves to reduce the actuation voltage [25], thus we chose a high dielectric material (HfO_2) to further assist in the actuation performance. Sensor integration into DMF platforms is an essential step for the advancement of biomedical applications. The reported embedded sensors are either complex or have constrained operations in the DMF system. While optical sensors are favored as the traditional diagnostic verification method, the integrated optic sensors that are reported on usually come with sophisticated systems that make them unfeasible for public use [26-29]. In the same way, thermal sensors generally have a limited use and are bulky [30]. Capacitive sensors are very popular in bioassays due to their simple structure, capability for integration, and reliable sensitivity and flexibility [31, 32]. These sensors are considered part of the impedance sensor, although many people confuse the former with the latter. While an impedance sensor inherently measures capacitance, it requires a fast sampling rate and is bound to much interferences during measurement [33]. On the other hand, the capacitive sensor reflects a mature technology and requires less complicated measurement setup. In this study we therefore opted to take advantage of the capacitive electrodes for actuation and sensing. During an infection or acute inflammation, a patient's C-reactive protein (CRP) production would normally be high.

The authors are with the Department of Computer, Electrical and Mathematical Sciences & Engineering, King Abdullah University Of Science and Technology, Thwual, 23955, Kingdom of Saudi Arabia (e-mail: yousof.mashraei@kaust.edu.sa; shilpa.sivashankar@kaust.edu.sa; ulrich.buttner@kaust.edu.sa; khaled.salama@kaust.edu.sa).

This article has been accepted for publication in a future issue of this journal, but has not been fully edited. Content may change prior to final publication. Citation information: DOI 10.1109/JSEN.2016.2578440, IEEE Sensors Journal

Detection of CRP beyond 3mg/L would certainly indicate that the patient requires medical assistance [34]. CRP can be quantified with a diagnostic blood-screening test. It has generated considerable attention, as it can provide a good indication of many health conditions, including heart diseases [35, 36]. Its value for detecting cardiovascular disease stems from the fact that it measures vascular inflammation [37]. In recent years, many efforts have been taken to minimize the time and increase the specificity of agglutination reaction, unlike enzyme-linked immunosorbent assay (ELISA). ELISA [38] on microtiter plates is tedious and time consuming; in addition, it is also limited by mass transfer kinetics. To overcome these problems, several attempts are made to switch agglutination onto a multiplexed tabletop LOC system that is easy and less time consuming. Apart from some visual methods (such as slides and cards) for qualitatively detecting the agglutination of sensitized particles, optical techniques to quantify the agglutination do exist. The most important techniques are turbidimetry [39], nephelometry [40], angular anisotropy, and photon correlation spectroscopy (light scattering measurements). Qualitative methods require larger particles than quantitative methods. In general, the particle diameter range for visual slide agglutination is 0.2μm-0.9μm, whereas it is 0.01μm-0.3μm for light scattering immunoassays. Furthermore, integration of turbidimetry or light scattering techniques is too feebly tailored to fit into micro and nanoscale quantifications. We have therefore made efforts to quantify CRP on a DMF platform. In this work, we propose the integration of a first two-terminal electrode into an open DMF platform. The proposed electrode is a fractal shape that provides improved actuation functionality and works as a capacitive biosensor. The fractal shape is a utilization of a Hilbert space-filling curve that fills up a definite area with a repetitive and continuous pattern [41]. The fractal shape is reported to have less residual stress as well as to provide a uniform distribution of the electrical field [42, 43]. The uniform electrical field distribution and prompted capacitance are the key factors of the improved DMF performance. The unique electrode structure introduces the possibility of big scale multiplexing biosensors, which would only require a simple pretreatment to the electrode's surface before the final release. That would bring the DMF platform closer to the point-of-care applications. DMF also reduces the process of diagnostics to a great extent by reducing the assay's protocol as well as time. Also, because of its miniaturized size, biomedical imaging and monitoring devices will be potential candidate for DMF integration [44].

II. THEORY AND SIMULATION

Droplet actuation is the primary function of the DMF. The EWOD is an effect that renders the hydrophobic surface to hydrophilic under an applied voltage. This behavior is in accordance with the Young-Lippmann equation [45], which is as follows:

$$\cos(\theta_0) - \cos(\theta_a) = \frac{C * V^2}{2 * \gamma_{LG}}$$

where (θ_0, θ_a) are the resting and actuating angles respectively, (γ_{LG}) is the gas-surface tension, (C) is the dielectric capacitance, and (V) is the applied voltage. From the equation, it is apparent that there are three possible ways to enhance the actuation performance: (1) increasing the applied voltage, (2) increasing the capacitance, and/or (3) decreasing the surface tension. However, as the surface tension is a material property, it is limited to the chosen material. Similarly, increasing voltage can cause several problems, such as dielectric failure and electrolysis of the droplet. Thus, introducing more capacitance to the system is more rational. The capacitance in the DMF system is determined by the materials of choice and the geometrical shape. So, the shape of the electrode can be better utilized by using a space-filling technique (such as fractal shapes) that introduces more capacitance to the system using the same electrode area, and hence, improve the performance. The added capacitance is due to the irregular shape which causes stray electrical fields on the surface. To validate this hypothesis, the electrical field of

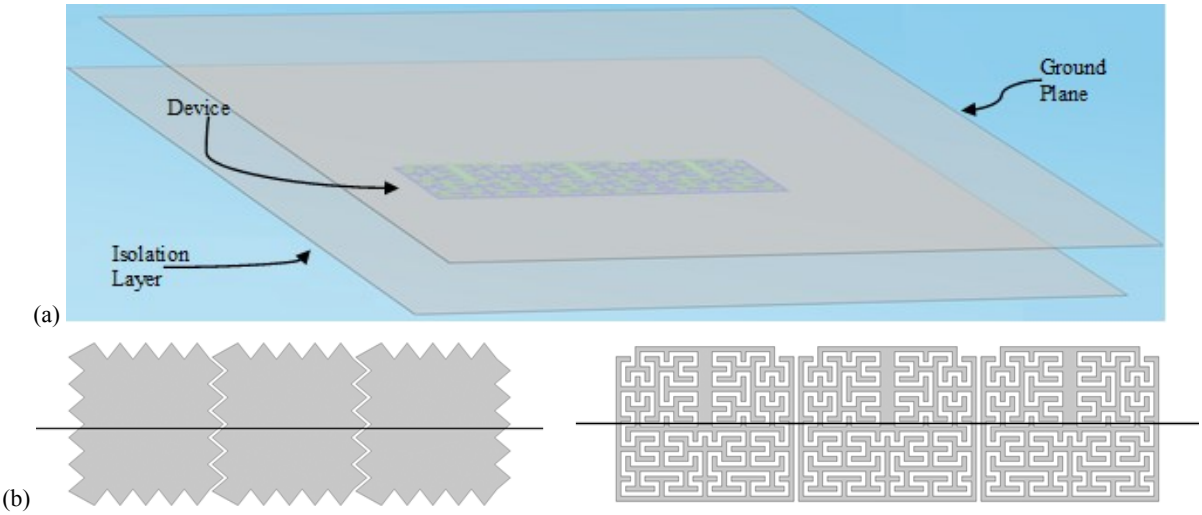

Fig. 1. (a) Device configuration in COMSOL Multiphysics. (b) The V-notch Square electrode (left) and Fractal electrode (right) with the evaluation cutline where the electric field is evaluated.

This article has been accepted for publication in a future issue of this journal, but has not been fully edited. Content may change prior to final publication. Citation information: DOI 10.1109/JSEN.2016.2578440, IEEE Sensors Journal

two electrode designs – namely (1) fractal and (2) V-notch shape – are simulated in COMSOL® Multiphysics v5.1 and compared in terms of electrical field uniformity and intensity. The electrical field is evaluated on the device's surface, as the EWOD occurs effectively at this interface between the device and the droplet. The first device, which is composed of three fractal electrodes, has an inner spacing of 3µm, spaced at 3µm from each other, and occupies an area of 111µm X 93µm. The second design has three V-notch electrodes of 100µm X 99µm that are 3µm apart. This area mismatch is due to the drawing limitations associated with distributing the V-notches equally apart from each other. Regardless, both devices are mounted on a 1µm isolation layer, and the ground plane is distanced 100µm above the electrodes. The voltage is kept at 100V, and the metal layer thickness of the electrodes is 100nm, as depicted in Fig.1(a). The simulation is carried out by activating the middle electrode and evaluating the voltage distribution on the surface, as well as the electrical field intensity along the evaluation cutline located at the center of the device, see Fig.1(b). The results show that fractal device has better electrical field distribution, which is the electrical potential developed across the device. The electrical field is found more uniform due to the charge accumulation in the fractal electrode, Fig.2(a). For that reason, the field intensity peaks in the fractal are diminished to about 50% of that in the V-notch square electrodes Fig.2(b), and consequently, the potential difference is lower, Table.1. These results predict several points. First; the accumulated charge on the fractal

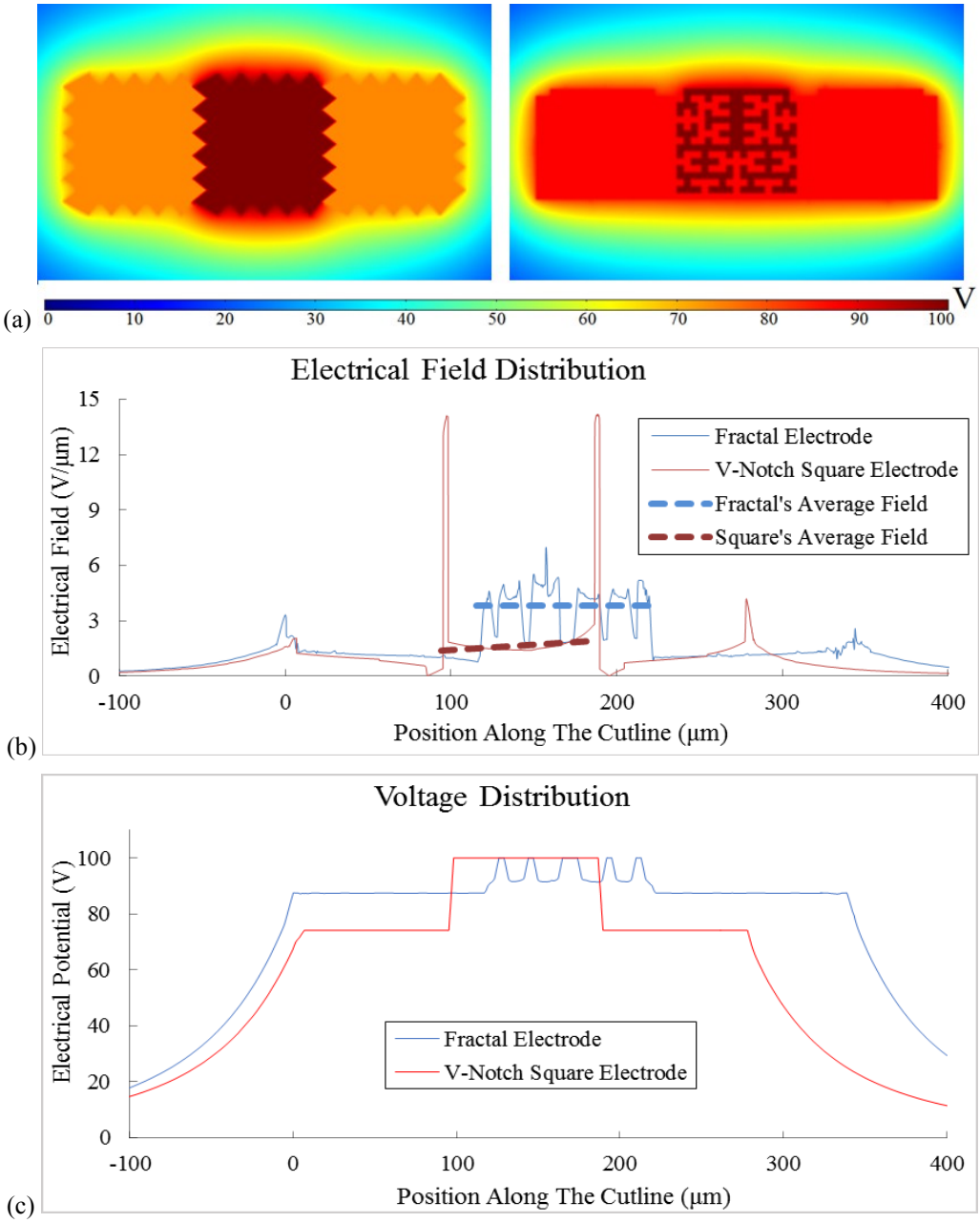

Fig. 2. (a) The distribution of the electrical potential across the device, (b) The electrical field evaluated along the cutline. Notice that the average fields are evaluated on the activated electrode as shown. (c) The induced electrical potential along the evaluation cutline.

This article has been accepted for publication in a future issue of this journal, but has not been fully edited. Content may change prior to final publication. Citation information: DOI 10.1109/JSEN.2016.2578440, IEEE Sensors Journal

electrodes, which will induce floating voltage, will facilitate the droplet motion. This induced voltage will reduce the contact angle on the whole droplet-electrode interface, not only on the edges of the electrode. This reduced contact angle isn't sufficient to actuate the droplet, but it reduces the energy needed for the actuation. In other words, the whole content of the droplet "slides" on the fractal electrode, rather than being "dragged" in typical electrode shapes. Second, the dielectric failure probability will be reduced significantly. The dielectric failure mainly happens as a result of the high potential difference between the electrodes, that causes high dielectric stress due to the shape effect [46, 47]. With the induced voltage on the other electrode, the potential difference will be lower, and hence, it'll reduce the dielectric stress. Thus, the durability of the fractal device will be increased. Also, using liquids with high surface tension coefficients is more viable because of the fractal's capability to withstand higher voltages. Third, this improvement is linked to the capacitance increase of the electrode. Because of the fractal shape, the stray capacitance is dominating the surface of the device. Since this stray capacitance is the main essence of the planar capacitive sensor, the electrode can be used for sensing as well as actuating simultaneously.

TABLE I
Comparison between Fractal and V-Notch Square Electrodes

Electrode Shape	Fractal	V-Notch Square
Average Electrical Field (V/μm)	3.8	2.3
Peak Electrical Field (V/μm)	7.0	14.2
Induced Electrical Potential (V)	87	74

III. 3. MATERIALS AND METHODS

A. SAMPLE SITES

Standard CRP test kits (ASI, Arlington) and human CRP serum (Pronac) were used in all of the experiments. The kits consist of beads coated with anti-CRP antibodies, analyte and azide buffer. All dilutions were made using this azide buffer. The 3-Mercaptopropioninc Acid (MPA), 1-Ethyl-3-(3-dimethylaminopropyl) carbodiimide (EDC) and N-hydroxysuccinimide (NHS) required for immobilization were purchased from Sigma.

B. FABRICATION PROCESS

The fabrication process follows an in-house procedure, as illustrated in Fig.3. It starts by submersing the wafer in a hot piranha solution that contains a mixture of hydrogen peroxide (H_2O_2) and sulfuric acid (H_2SO_4) for about 10 minutes. The wafer is then washed with distilled water and dried in a nitrogen drier before being put in a furnace to thermally grow a 2μm-thick isolation layer of silicon dioxide (SiO_2). The metal layer is deposited by sputtering at 5mTorr vacuum with 400Wdc energy, which forms the conductive layer of 10nm titanium (Ti) and 100nm platinum (Pt). This layer is patterned by a photolithography process to expose the metal layer underneath. A dry etch process utilizing argon (Ar) gas at 300W plasma power for 10 minutes is next used to etch the exposed metal to form the active devices. The photoresist is then stripped off using an acetone and IPA wash before plasma-descum to ensure the removal of all the residues. The dielectric layer is then deposited by Atomic Layer Deposition (ALD) for 1000 cycle at 300°C and 80mTorr to form a 150nm hafnium dioxide (HfO_2) layer. Then, a Teflon layer was spin coated on the device at 2000rpm and baked at 160°C for 30 minutes to provide the hydrophobic surface needed for the actuation. The Fractal electrode design has an inner spacing of 6μm. Both fractal and V-notch square electrodes have 4.84mm^2 size area and a 60μm separation distance between electrodes. The fabricated devices are mounted on a chip of 17mm X 14mm size area.

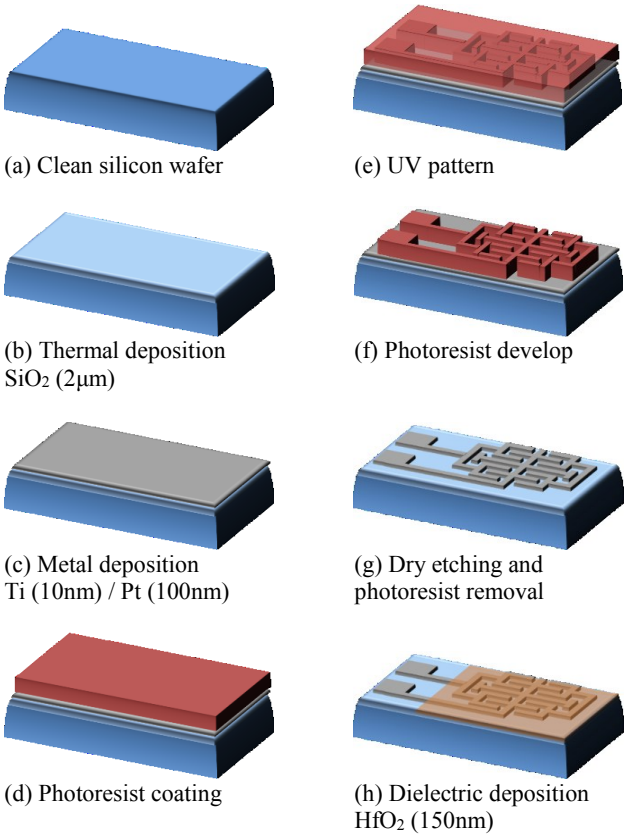

Fig. 3. Fabrication process for the fractal-electrode device.

C. HOLDER FABRICATION

A special holder was designed to secure the chip in place and have a proper connection with the instruments, see Fig.4. It is made out of polymethylmethacrylate (PMMA) and laser-cut into two parts: chip restrainer and clips holder. The chip restrainer has 14 slots for pogo pins and four screw holes. The pogo pins slots are deliberately distanced to match the actual locations of the pads; the pins are consequently glued tightly into these slots. The clips holder has three sidewalls and a base. The sidewalls have slots to fit the LabSmith Micro-Clips that clamp firmly to the pogo pins, while the base has a slot to

This article has been accepted for publication in a future issue of this journal, but has not been fully edited. Content may change prior to final publication. Citation information: DOI 10.1109/JSEN.2016.2578440, IEEE Sensors Journal

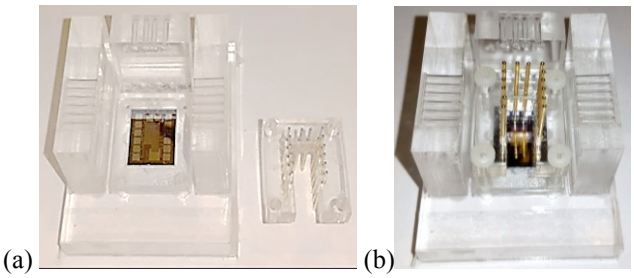

(a) (b)

Fig. 4. (a) Laser-fabricated holder for probing electrodes, (b) The holder after assembly.

securely hold the chip and contains four screw holes. The whole system is tightened during the measurement with screws.

D. IMMOBILIZATION

The immobilization of antibodies is an important step in the CRP concentration test. The process consists of three major steps, as illustrated in Fig.5. Firstly, during Teflon coating, selected fractal electrodes are covered by Kapton® tape for the surface treatment. After coating the Teflon layer, the Kapton tapes are taken off and these fractal electrodes are cleaned and then immersed in an ethanolic solution of 10mM MPA for 24hrs. They are next washed with distilled water and allowed to dry. Secondly, they are treated with a solution containing 0.05M EDC and 0.03M NHS for 4hrs to form self-assembled monolayers (SAM). Thirdly, 2µl of CRP antibodies are added and allowed to settle on the surface for 1hr. They are then washed with distilled water to remove any unattached antibodies.

E. CRP PREPARATION

Biomedical assays are widely reported in the DMF platform. Immunoagglutination or passive agglutination is considered to be one-step assay and is therefore used in biomedical applications. Commercially available CRP proteins are diluted with azide buffer. The prepared concentrations of the CRP are 0.5mg/L, 2.0mg/L, and 6.0mg/L. The concentration of immobilized beads was 1.0mg/ml and hence 2µl of these beads were added to immobilize on the surface of the sensors. A sufficient number of beads to cover the sensor area was added and allowed to settle for about 1hr before the sensor was washed with distilled water to remove any attached beads. Studies reveal a link between CRP concentrations and the risk of patients who are prone to cardiac diseases. Based on the concentration of CRP present in the sample, three different levels of patient's risk can be assessed; low risk (below 1mg/L), medium risk (1-3mg/L) and high risk (above 3mg/L). We hence chose the aforementioned concentration samples to cover all risk levels. The samples were diluted with the commercially available azide buffer to avoid CRP denaturation during the sample handling process.

IV. RESULTS AND DISCUSSION

A. Actuation Test

After placing the chip in the holder, the LabSmith High Voltage Sequencer is connected to the chip through the micro-clips and controlled by a laptop. The sequencer generates high voltages and provides feedback readouts of the applied voltage-current on the pads. The test employs the open DMF configuration by grounding one set-line of electrodes and activating the desired terminals on the other. As found in the simulation results, the 2-terminal fractal electrode is tested by activating one terminal and keeping the other terminal float. This configuration will keep the complexity of the wiring on the same level to the conventional 1-terminal electrode system, and thus will work similarly in that perspective.

A responsive actuation of a 20µl water droplet was observed at an applied voltage of 100V using the fractal-electrode device, as illustrated in Fig.6 (a-h). As expected from the simulation results, the droplet-electrode interface is

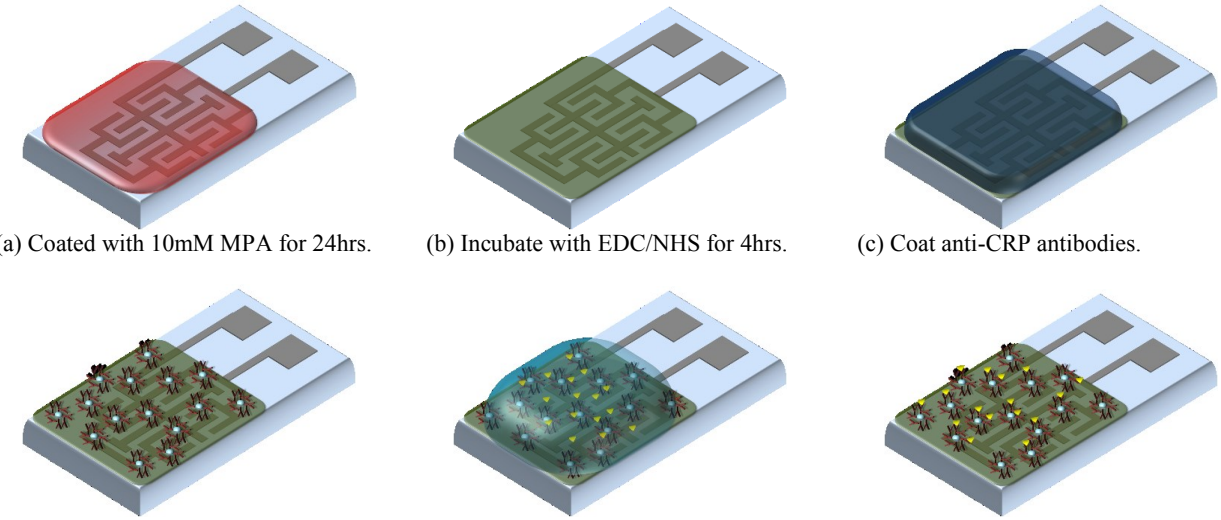

(a) Coated with 10mM MPA for 24hrs. (b) Incubate with EDC/NHS for 4hrs. (c) Coat anti-CRP antibodies.

(d) Immobilized anti-CRP antibodies. (e) Add the human CRP serum (f) Attachment of the CRP to the antibodies.

Fig. 5. Schematic representation of immobilizing anti-CRP antibodies.

This article has been accepted for publication in a future issue of this journal, but has not been fully edited. Content may change prior to final publication. Citation information: DOI 10.1109/JSEN.2016.2578440, IEEE Sensors Journal

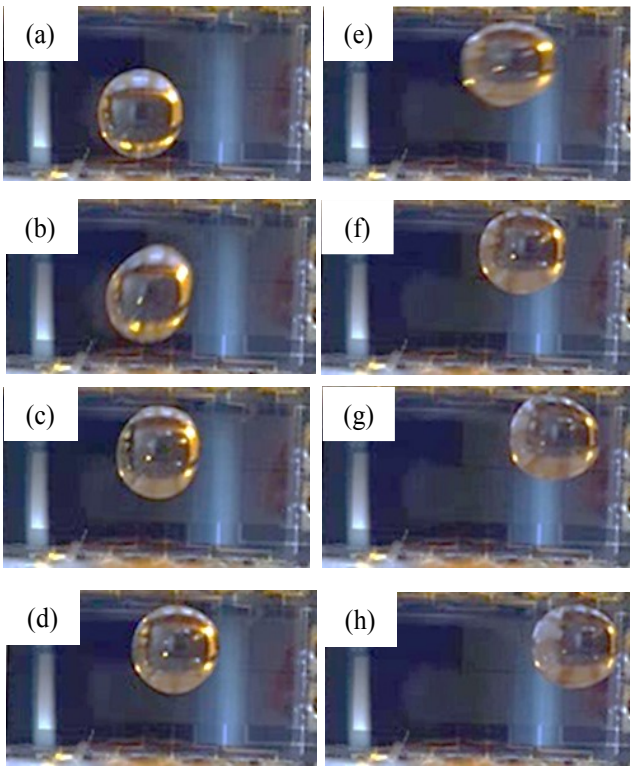

Fig. 6. (a-h): Image sequence showing a droplet actuation in a fractal electrode device.

experiencing about the same reduction in contact angle that facilitate the motion. However with the V-notch square electrode device, the 20µl droplet didn't actuate under the applied voltage, and only pulsated on the spot. The volume of the droplet was increased to 30µl to cover bigger area, and a typical dragging motion was observed with 100V. Unlike the fractal electrode, the contact angle in the V-notch square electrode is reduced more on the edges that hinder the droplet motion.

B. EFFECTIVE DIELECTRIC STRENGTH MEASUREMENT

The effective dielectric strength of the fabricated devices is evaluated using the same configuration in the actuation test. The voltage was gradually increased on the tested electrode while obtaining its I-V characteristics. The breakdown voltage

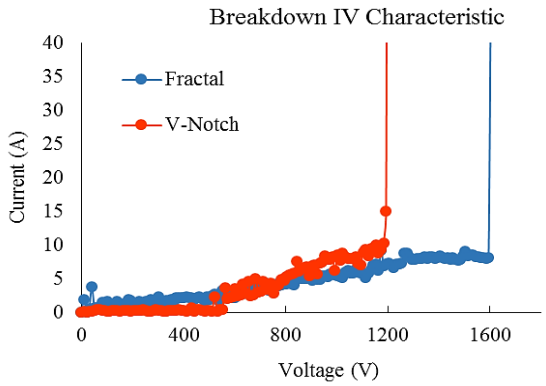

Fig. 7. I-V characteristics of the fractal and V-notch square electrodes.

is taken when the current value shoots abruptly to the preset high limit. The LabSmith High Voltage Sequencer is used to generate the voltage and then measure the voltage and current on the selected electrodes at the same time. The results show an improvement of the effective dielectric strength of about 33% in the fractal-electrode that elevated the breakdown voltage to 1600V, as depicted in Fig.7. As shown in the simulation, the reduced field intensity peaks between the fractal electrodes are linked to the higher breakdown voltage on the fractal.Though both devices have the same dielectric, the V-notch square electrode experiences a higher electrical potential difference, and thus, is more likely to dielectric breakdown failures. This high voltage tolerance in fractal electrodes will permit the use of different liquids in DMF platforms, with less concern about their contact angle.

C. CRP QUANTIFICATION

Passive agglutination is a process in which antibodies are first coated onto latex support and then combined with antigen to see agglutination. One of its applications is the detection of CRP which is produced by the liver. All methods of detecting or quantifying an antigen or antibody take advantage of the fact that they react to form complexes; this is something that is specific to CRP. At the optimum antigen-antibody concentration, these complexes precipitate out. However, if an antigen is specific in nature, agglutination of the antigen-antibody complex is observed. To quantify CRP proteins, two sensors were employed: (1) untreated fractal electrodes, and (2) surface-treated fractal electrodes "biosensors." When we used the untreated fractal electrode, not much difference in capacitance readouts were observed with different concentrations; we thus had to undertake the surface treatment procedure. When the sensors were immobilized with anti-CRP antibodies, we could see the clear quantification of the given samples. CRP proteins were diluted to concentrations of 0.5mg/L, 2mg/L and 6mg/L. These are the quantified concentrations that were chosen by American Heart Association (AHA) as the limits for assessing the risk of cardiac diseases. To quantify these concentrations, 2µl of the proteins diluted with azide buffer were added on the immobilized surface and measured using the Agilent E4980A Precision LCR Meter through the control unit. The capacitance was measured at 1kHz for approximately 15 minutes; it is plotted in Fig.8(a). The capacitance decreased as the concentration of the serum proteins increased. The limit of detection (LOD) test is performed by adding different concentrations to the biosensor, from as low as 0.25mg/L to 10mg/L. The ratio of increase in capacitance with concentration is shown in Fig.8(b). From this figure, it is evident that the ratio of increase in capacitance was decreasing with the increase in concentration. The ratio increase was around 214 times for a concentration of 0.25mg/L, and decreased to around 7 times for a concentration of 10mg/L, which confirms that the sensors were able to quantify a given sample. The biosensor measurements showed a response in capacitance within 3 minutes, which indicates a high sensitivity to CRP concentrations. However, the capacitance

This article has been accepted for publication in a future issue of this journal, but has not been fully edited. Content may change prior to final publication. Citation information: DOI 10.1109/JSEN.2016.2578440, IEEE Sensors Journal

level has an inverse relationship to the concentrations. This phenomenon can be interpreted as a dielectric reduction due to more antigen-antibody interactions. The capacitance tends to stabilize with time as a result of the agglutination complex that is being formed with time. Untreated fractal electrode measurements showed no significant sensitivity to the CRP concentrations as the capacitance was slightly dropped. This result suggests that the antibody-immobilization step is crucial to CRP quantification.

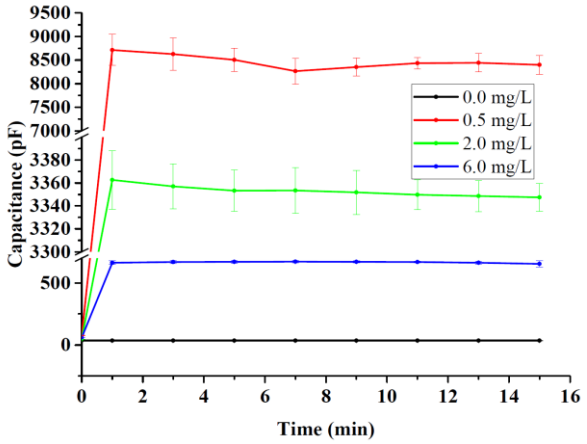

(a)

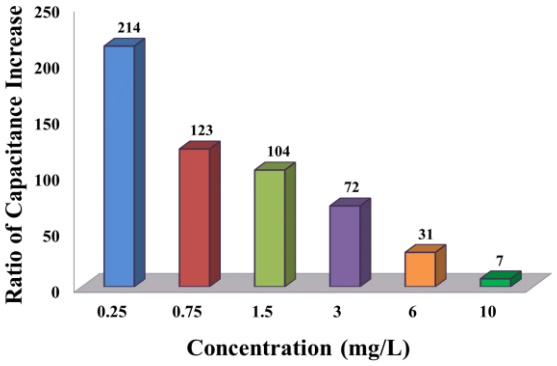

(b)

Fig. 8. (a) CRP quantified as per the limits set by the AHA. (b) The ratio increase in the capacitance with varying the concentration of the CRP. The ratio tends to decrease as the concentration increases.

V. CONCLUSIONS

A successful integration of a fractal electrode biosensor in a simple DMF system is reported in this work. The improved performance is validated by a simulation comparison of the electrical field between the fractal and V-notch electrodes. A responsive droplet actuation is observed in the fractal electrodes with no dragging behavior. The droplet dragging usually is caused by the unbalanced contact angles at the droplet-electrode interface, which resulted in hindered motion of the droplet. With a uniform electrical field in the fractal electrode, the droplet is sliding on the electrodes and hence the voltage has efficiently actuated the droplet. For that reason, the effective dielectric strength is improved in the fractal electrode by a 33% increase of the breakdown voltage when compared to the V-notch square electrode. The fractal electrode is capable of capacitive sensing because of its structure. Selected fractal electrodes are transformed easily into CRP biosensors by a surface treatment procedure. The biosensor result shows a CRP response that is sensitive but has a decreasing sensitivity-trend as the CRP concentration increases. Untreated fractal electrodes measurement shows no significant response. The fractal electrode is an economical choice for future development of technology. Although the fractal electrode introduces several advantages, a potential drawback is the number of pads required for each electrode. That might be problematic for routing the connection wires in a big sophisticated system. Nonetheless, different biosensors can be selectively added to the DMF platform with simple processes. It can also provide feedback signals to improve the automation of the process besides lengthening the durability of the device.

REFERENCES

[1] M. Pandiaraj, A. R. Benjamin, T. Madasamy, K. Vairamani, A. Arya, N. K. Sethy, *et al.*, "A cost-effective volume miniaturized and microcontroller based cytochrome c assay," *Sensors and Actuators A: Physical,* vol. 220, pp. 290-297, 2014.

[2] T. H. Khan, R. Shrestha, K. A. Wahid, and P. Babyn, "Design of a smart-device and FPGA based wireless capsule endoscopic system," *Sensors and Actuators A: Physical,* vol. 221, pp. 77-87, 2015.

[3] M. Venugopal, S. K. Arya, G. Chornokur, and S. Bhansali, "A realtime and continuous assessment of cortisol in ISF using electrochemical impedance spectroscopy," *Sensors and Actuators A: Physical,* vol. 172, pp. 154-160, 2011.

[4] R. B. Fair, "Digital microfluidics: is a true lab-on-a-chip possible?," *Microfluidics and Nanofluidics,* 2007.

[5] P. T. Kumar, F. Toffalini, D. Witters, S. Vermeir, F. Rolland, M. L. Hertog, *et al.*, "Digital microfluidic chip technology for water permeability measurements on single isolated plant protoplasts," *Sensors and Actuators B: Chemical,* vol. 199, pp. 479-487, 2014.

[6] Y.-J. Liu, D.-J. Yao, H.-C. Lin, W.-Y. Chang, and H.-Y. Chang, "DNA ligation of ultramicro volume using an EWOD microfluidic system with coplanar electrodes," *Journal of Micromechanics and Microengineering,* vol. 18, p. 045017, 2008.

[7] N. Vergauwe, S. Vermeir, J. B. Wacker, F. Ceyssens, M. Cornaglia, R. Puers, *et al.*, "A highly efficient extraction protocol for magnetic particles on a digital microfluidic chip," *Sensors and Actuators B: Chemical,* vol. 196, pp. 282-291, 2014.

[8] M. Abdelgawad and A. R. Wheeler, "The digital revolution: a new paradigm for microfluidics," *Advanced Materials,* vol. 21, pp. 920-925, 2009.

[9] J. Gong and C.-J. Kim, "Direct-referencing two-dimensional-array digital microfluidics using multilayer printed circuit board," *Microelectromechanical Systems, Journal of,* vol. 17, pp. 257-264, 2008.

[10] G. J. Shah and C.-J. C. Kim, "Meniscus-assisted high-efficiency magnetic collection and separation for EWOD droplet microfluidics," *Microelectromechanical Systems, Journal of,* vol. 18, pp. 363-375, 2009.

[11] B. Hadwen, G. R. Broder, D. Morganti, A. Jacobs, and C. Brown, "Programmable large area digital microfluidic array with integrated droplet sensing for bioassays," *Lab on a Chip,* 2012.

[12] J. Zeng, "Modeling and simulation of electrified droplets and its application to computer-aided design of digital microfluidics," *Computer-Aided Design of Integrated Circuits and Systems, IEEE Transactions on,* vol. 25, pp. 224-233, 2006.

[13] T. Xu, K. Chakrabarty, and F. Su, "Defect-aware high-level synthesis and module placement for microfluidic biochips," *Biomedical Circuits and Systems, IEEE Transactions on,* vol. 2, pp. 50-62, 2008.

[14] T. Xu, K. Chakrabarty, and V. K. Pamula, "Defect-tolerant design and optimization of a digital microfluidic biochip for protein crystallization," *Computer-Aided Design of Integrated Circuits and Systems, IEEE Transactions on,* vol. 29, pp. 552-565, 2010.

[15] P. Pop, M. Alistar, E. Stuart, and J. Madsen, *Fault-Tolerant Digital Microfluidic Biochips: Compilation and Synthesis*: Springer, 2015.

[16] S.-T. Yu, S.-H. Yeh, and T.-Y. Ho, "Reliability-driven chip-level design for high-frequency digital microfluidic biochips," *Computer-Aided Design of Integrated Circuits and Systems, IEEE Transactions on,* vol. 34, pp. 529-539, 2015.

[17] C.-Y. Huang, P.-H. Shih, P.-Y. Tsai, I. Lee, H.-Y. Hsu, H.-Y. Huang*, et al.*, "AMPFLUID: Aggregation Magnified Post-Assay Fluorescence for Ultrasensitive Immunodetection on Digital Microfluidics," *Proceedings of the IEEE,* vol. 103, pp. 225-235, 2015.

[18] M. J. Schertzer, R. Ben Mrad, and P. E. Sullivan, "Automated detection of particle concentration and chemical reactions in EWOD devices," *Sensors and Actuators B: Chemical,* vol. 164, pp. 1-6, 3/31/ 2012.

[19] R. Sista, Z. Hua, P. Thwar, A. Sudarsan, and V. Srinivasan, "Development of a digital microfluidic platform for point of care testing," *Development of a digital microfluidic platform for point of care testing,* 2008.

[20] M. Ahamedi, R. Ben-Mrad, and P. Sullivan, "Electrowetting on Dielectric (EWOD)-based thermo-responsive microvalve for interfacing droplet flow with continuous flow," *Microelectromechanical Systems, Journal of,* vol. 22, pp. 536-541, 2013.

[21] I. A. Eydelnant, B. B. Li, and A. R. Wheeler, "Microgels on-demand," *Nature communications,* vol. 5, 2014.

[22] S. K. Cho, S.-K. Fan, H. Moon, and C.-J. Kim, "Towards digital microfluidic circuits: creating, transporting, cutting and merging liquid droplets by electrowetting-based actuation," in *Micro Electro Mechanical Systems, 2002. The Fifteenth IEEE International Conference on*, 2002, pp. 32-35.

[23] S. C. Shih, I. Barbulovic-Nad, X. Yang, R. Fobel, and A. R. Wheeler, "Digital microfluidics with impedance sensing for integrated cell culture andanalysis," *Biosensors and Bioelectronics,* vol. 42, pp. 314-320, 2013.

[24] J. K. Park, S. J. Lee, and K. H. Kang, "Fast and reliable droplet transport on single-plate electrowetting on dielectrics using nonfloating switching method," *Biomicrofluidics,* vol. 4, p. 024102, 2010.

[25] S. Sohail, E. A. Mistri, A. Khan, S. Banerjee, and K. Biswas, "Fabrication and performance study of BST/Teflon nanocomposite thin film for low voltage electrowetting devices," *Sensors and Actuators A: Physical,* vol. 238, pp. 122-132, 2016.

[26] M. W. Royal, N. M. Jokerst, and R. B. Fair, "Droplet-based sensing: optical microresonator sensors embedded in digital electrowetting microfluidics systems," *Sensors Journal, IEEE,* vol. 13, pp. 4733-4742, 2013.

[27] L. Luan, R. D. Evans, N. M. Jokerst, and R. B. Fair, "Integrated optical sensor in a digital microfluidic platform," *Sensors Journal, IEEE,* vol. 8, pp. 628-635, 2008.

[28] M. W. Royal, N. M. Jokerst, and R. B. Fair, "Integrated sample preparation and sensing: Polymer microresonator sensors embedded in digital electrowetting microfluidic systems," *Photonics Journal, IEEE,* vol. 4, pp. 2126-2135, 2012.

[29] P. Shao Ning, J. K. Valley, W. Yi-Lun, and M. C. Wu, "Distributed Circuit Model for Multi-Color Light-Actuated Opto-Electrowetting Microfluidic Device," *Lightwave Technology, Journal of,* vol. 33, pp. 3486-3493, 2015.

[30] A. R. McLanahan and C. D. Richards, "A dielectric liquid contact thermal switch with electrowetting actuation," *A dielectric liquid contact thermal switch with electrowetting actuation,* 2011.

[31] S. Sivashankar, C. Sapsanis, U. Buttner, and K. N. Salama, "Flexible low-cost cardiovascular risk marker biosensor for point-of-care applications," *Electronics Letters,* vol. 51, pp. 1746-1748, 2015.

[32] M. J. Schertzer, R. Ben-Mrad, and P. E. Sullivan, "Using capacitance measurements in EWOD devices to identify fluid composition and control droplet mixing," *Sensors and Actuators B: Chemical,* vol. 145, pp. 340-347, 3/4/ 2010.

[33] T. Lederer, S. Clara, B. Jakoby, and W. Hilber, "Integration of impedance spectroscopy sensors in a digital microfluidic platform," *Microsystem technologies,* vol. 18, pp. 1163-1180, 2012.

[34] P. M. Ridker, E. Danielson, F. Fonseca, J. Genest, A. M. Gotto Jr, J. Kastelein*, et al.*, "Rosuvastatin to prevent vascular events in men and women with elevated C-reactive protein," *New England Journal of Medicine,* vol. 359, p. 2195, 2008.

[35] Y.-N. Yang, H.-I. Lin, J.-H. Wang, S.-C. Shiesh, and G.-B. Lee, "An integrated microfluidic system for C-reactive protein measurement," *Biosensors and Bioelectronics,* vol. 24, pp. 3091-3096, 2009.

[36] W.-B. Lee, Y.-H. Chen, H.-I. Lin, S.-C. Shiesh, and G.-B. Lee, "An integrated microfluidic system for fast, automatic detection of C-reactive protein," *Sensors and Actuators B: Chemical,* vol. 157, pp. 710-721, 2011.

[37] K. Sato, M. Tokeshi, H. Kimura, and T. Kitamori, "Determination of carcinoembryonic antigen in human sera by integrated bead-bed immunoasay in a microchip for cancer diagnosis," *Analytical Chemistry,* vol. 73, pp. 1213-1218, 2001.

[38] M. Özdemir, B. Feyzioğlu, M. G. Kurtoğlu, M. Doğan, H. T. Dağı, Ş. Yüksekkaya*, et al.*, "A comparison of immuncapture agglutination and ELISA methods in serological diagnosis of brucellosis," *International journal of medical sciences,* vol. 8, p. 428, 2011.

[39] D. W. Kim, P. E. Kilgore, E. J. Kim, S. A. Kim, D. D. Anh, and M. Seki, "Loop-mediated isothermal amplification assay for detection of Haemophilus influenzae type b in cerebrospinal fluid," *Journal of clinical microbiology,* vol. 49, pp. 3621-3626, 2011.

[40] F. J. Gella, J. Serra, and J. Gener, "Latex agglutination procedures in immunodiagnosis," *Pure and applied chemistry,* vol. 63, pp. 1131-1134, 1991.

[41] B. Moon, H. V. Jagadish, C. Faloutsos, and J. H. Saltz, "Analysis of the clustering properties of the Hilbert space-filling curve," *Knowledge and Data Engineering, IEEE Transactions on,* vol. 13, pp. 124-141, 2001.

[42] A. M. Elshurafa, P. Ho, and K. N. Salama, "Modeling and fabrication of an RF MEMS variable capacitor with a fractal geometry," in *Circuits and Systems (ISCAS), IEEE International Symposium on 2013* 2013, pp. 2711-2714.

[43] A. M. Elshurafa, A. G. Radwan, A. Emira, and K. N. Salama, "RF MEMS fractal capacitors with high self-resonant frequencies," *Microelectromechanical Systems, Journal of,* vol. 21, pp. 10-12, 2012.

[44] S. Sukhatme and A. Agarwal, "Digital microfluidics: Techniques, their applications and advantages," *Journal of Bioengineering & Biomedical Science,* vol. 2013, 2012.

[45] S. K. Cho, H. Moon, and C.-J. Kim, "Creating, transporting, cutting, and merging liquid droplets by electrowetting-based actuation for digital microfluidic circuits," *Microelectromechanical Systems, Journal of,* vol. 12, pp. 70-80, 2003.

[46] M. Hanai, T. Nakamoto, and H. Ikeda, "Dielectric breakdown characteristics of an insulator with a sharp edge in SF6 gas under lightning impulse voltage," *Dielectrics and Electrical Insulation, IEEE Transactions on,* vol. 14, pp. 321-327, 2007.

[47] T. Mukherjee and A. Paul, "Dielectric Breakdown-Assisted Corona Discharge-Based Pressure Sensor Using Poly-Si Microtips," *IEEE Transactions on Electron Devices,* vol. 63, pp. 2080-2088, 2016.